



Research article

Investigation the apoptotic effect of silver nanoparticles (Ag-NPs) on MDA-MB 231 breast cancer epithelial cells via signaling pathways

Soheila Montazersaheb^{a,*,1}, Raheleh Farahzadi^b, Ezzatollah Fathi^c,
Mahsan Alizadeh^d, Shahabaddin Abdolalizadeh Amir^d, Alireza Khodaei Ardakan^e,
Sevda Jafari^{f,1,**}

^a Molecular Medicine Research Center, Tabriz University of Medical Sciences, Tabriz, Iran

^b Hematology and Oncology Research Center, Tabriz University of Medical Sciences, Tabriz, Iran

^c Department of Clinical Sciences, Faculty of Veterinary Medicine, University of Tabriz, Tabriz, Iran

^d Department of Clinical Sciences, Faculty of Veterinary Medicine, Tabriz Medical Sciences, Islamic Azad University, Tabriz, Iran

^e Faculty of Veterinary Medicine, Islamic Azad University, Science and Research Branch, Tehran, Iran

^f Nutrition Research Center, Tabriz University of Medical Sciences, Tabriz, Iran

ARTICLE INFO

Keywords:

Ag-NPs

MDA-MB 231 cell line

Anti-cancer

Apoptosis

Signaling pathways

ABSTRACT

Background: The discovery of novel cancer therapeutic strategies leads to the development of nanotechnology-based methods for cancer treatment. Silver nanoparticles (Ag-NPs) have garnered considerable interest owing to their size, shape, and capacity to modify chemical, optical, and photonic properties. This study aimed to investigate the impact of Ag-NPs on inducing of apoptosis in MDA-MB 231 cells by examining specific signaling pathways.

Materials and methods: The cytotoxicity of Ag-NPs was determined using an MTT assay in MDA-MB 231 cells. The apoptotic effects were assessed using the Annexin-V/PI assay. Real-time PCR and western blotting were conducted to analyze the expression of apoptosis-related genes and proteins, respectively. Levels of ERK1/2 and cyclin D1 were measured using ELISA. Cell cycle assay was determined by flow cytometry. Cell migration was evaluated by scratch assay.

Results: The results revealed that Ag-NPs triggered apoptosis and cell cycle arrest in MDA-MB 231 cells. The expression level of Bax (pro-apoptotic gene) was increased, while Bcl-2 (anti-apoptotic gene) expression was decreased. Increased apoptosis was correlated with increased levels of p53 and PTEN. Additionally, notable alterations were observed in protein expression related to the Janus kinase/Signal transducers (JAK/STAT) pathway, including p-AKT. Additionally, reduced expression of h-TERT was observed following exposure to Ag-NPs. ELISA results demonstrated a significant reduction in p-ERK/Total ERK and cyclin D1 levels in Ag-NPs-exposed MDA-MB 231 cells. Western blotting analysis also confirmed the reduction of p-ERK/Total ERK and cyclin D1. Decreased level of cyclin D is associated with suppression of cell cycle progression. The migratory ability of MDA-MB-231 cells was reduced upon treatment with Ag-NPs.

* Corresponding author. Molecular Medicine Research Center, Tabriz University of Medical Sciences, Tabriz, Iran.

** Corresponding author. Nutrition Research Center, Tabriz University of Medical Sciences, Tabriz, Iran.

E-mail addresses: montazersahebs@tbzmed.ac.ir (S. Montazersaheb), Jafarise@tbzmed.ac.ir (S. Jafari).

¹ These authors contributed equally to this work.

<https://doi.org/10.1016/j.heliyon.2024.e26959>

Received 6 August 2023; Received in revised form 29 January 2024; Accepted 22 February 2024

Available online 26 February 2024

2405-8440/© 2024 The Authors. Published by Elsevier Ltd. This is an open access article under the CC BY-NC-ND license (<http://creativecommons.org/licenses/by-nc-nd/4.0/>).

Conclusions: Our findings revealed that Ag-NPs influenced the proliferation, apoptosis, cell cycle, and migration in MDA-MB 231 cells, possibly by modulating protein expression of the AKT/ERK/Cyclin D1 axis.

1. Introduction

Cancer is a serious global health problem and is the second leading cause of mortality worldwide. The interplay between environmental and genetic factors intricately contributes to cancer development. Its hallmark lies in uncontrolled cell proliferation that leads to the destruction of surrounding tissues [1,2]. Surgery, chemotherapy, radiotherapy, immunotherapy, and hormonal therapy are traditional cancer treatments but often result in undesirable effects [3]. Among cancers affecting women, breast cancer is one of the most prevalent, accounting for 23 % of reported cancer cases. Within breast cancers, triple negative breast cancer (TNBC) represents about 15–20% of cases, characterized by more aggressive biology, distinct tumor phenotypes, and high recurrence rates. TNBC is defined by the absence of expression of estrogen receptor (ER), progesterone receptor (PR), and human epidermal growth factor 2 receptor (HER2). Approximately 12%–20% of all breast cancer cases belong to the TNBC phenotype (ER⁻/PR⁻/HER2⁻). The treatment landscape for TNBC is challenging due to the absence of specific receptors used in hormonal therapy. In other words, TNBC patients cannot benefit from conventional therapy or other targeted modalities employed for other breast cancer subtypes. Nanoparticles (NPs) have emerged as a promising alternative platform for treating TNBC [4,5].

A nanoparticle is specifically defined as a material with a size less than 100 nm [6]. Nanotechnology-based methodologies offer a means to mitigate systemic toxicity by employing functionalized moieties or biosynthesized nanocomposites like Fe₃O₄/Ag [7]. These nanoparticles exhibit unique properties, including tiny size, large surface-area-to-mass ratio, and high reactivity. These features present promising avenues for developing high-precision materials to overcome therapeutic and diagnostic barriers [8]. Silver nanoparticles (Ag-NPs) hold a prominent commercial status among nanomaterials due to their well-established antiseptic properties. In vitro experiments were used to investigate the properties, mechanisms of action and differential responses of Ag-NPs. Therefore, Ag-NPs are used as a novel candidate for therapeutic applications in cancer therapy [9]. The medical applications of Ag-NPs include drug delivery vectors, antibacterial agents, theranostic agents, and stem cell differentiation [10]. Ag-NPs possess the capability to induce oxidative stress, alter mitochondrial membrane, cause DNA damage, trigger apoptotic cell death, and prompt cytokine production [11]. In addition, it has been observed that Ag-NPs elicit a range of toxic effects, including alterations in oxidative stress-related genes and lipid peroxidation [12,13]. Despite this, limited studies have scrutinized the effects of Ag-NPs on breast cancer cell lines. In this study, we analyzed the apoptotic effects of Ag-NPs on MDA-MB 231 cells, serving as a model for human breast cancer. Our analysis aimed to determine the AKT (also known Protein kinase B), phosphatase and tensin homolog (PTEN), and P53 signaling pathways, recognized as pivotal signaling molecules activated in TNBC. The PI3K/AKT signaling pathway plays a crucial role in the growth, proliferation, angiogenesis, migration, and survival in TNBC. Notably, these pathways are remarkably upregulated in TNBC [14]. PTEN functions as a crucial tumor suppressor by inhibiting cell growth and increasing cellular susceptibility to apoptosis. Specifically, PTEN acts as a negative regulator of AKT activation; therefore, its function is lost upon AKT activation [15]. The role of telomerase reverse transcriptase (hTERT) was examined. hTERT is prominently overexpressed in most cancer cells and contributes significantly to cell proliferation [16].

ERK1 and ERK2 are integral components in the Ras-Raf-MEK-ERK signaling cascade, regulating cellular events such as proliferation, survival, differentiation, and cell cycle progression [17]. Upon activation, ERK1/2 translocates to the nucleus for phosphorylating transcription factors and promoting cell proliferation through the expression of cyclin D1 [18]. Cyclin D1 orchestrates the G1-S transition during the cell cycle. Indeed, cyclin D1 acts downstream from p-ERK; and its induction necessitates sustained ERK activation. Overexpression of cyclin D1 has been confirmed in many cancer cells, correlating with unfavorable prognoses [19]. This study aims to elucidate the effect of Ag-NPs on the induction of apoptotic signaling pathways.

2. Materials and Methods

Cell culture plates were provided by SPL Life Sciences (Pocheon, South Korea). Other cell culture materials were purchased from Gibco Co. (UK). The used Ag-NPs were synthesized by US Research Nanomaterials Inc. and purchased from the Iranian Nanomaterial Pioneers Company (Mashhad City, Khorasan, Iran).

2.1. Ag-NPs preparation

Distilled water was used to disperse polyvinylpyrrolidone (PVP)-coated Ag-NPs powder without adding surfactants. The size of the Ag-NPs measured between 50 and 80 nm with a purity of 99% [20]. The scanning electron microscopy analysis was validated by the Iranian Nanotechnology Initiative Council. Additionally, zeta potential and size distribution were provided by the commercial supplier, as reported in our previous study [20].

2.2. Cell culture of MDA-MB-231 cells

The MDA-MB-231 cell line served as a TNBC model. These cells were obtained from the Pasteur Institute of Iran and cultivated in

RPMI 1640 medium supplemented with 10% fetal bovine serum (FBS) and 100U/ml penicillin/streptomycin. MDA-MB-231 cells were cultured at a density of 15×10^4 cells/cm², incubated in a 5% CO₂ incubator under a humidified atmosphere at 37 °C, and passaged twice a week. The logarithmic growth phase of MDA-MB-231 was subjected to subsequent analysis.

2.3. Determination of cell viability

The viability of Ag-NP-treated cells was evaluated using an MTT-based colorimetric test. The assay relies on the reduction of MTT 3-(4,5-Dimethylthiazol-2-yl)-2,5-Diphenyltetrazolium Bromide (Sigma-Aldrich, USA) into water-insoluble purple formazan crystal that is formed by viable cells. In detail, 3×10^3 cells/well were seeded onto a 96-well plate. After 24 h, the cells were exposed to varying concentrations of Ag-NP (ranging from 0.1 to 7. µg/ml) and incubated for 48 h. Next, MTT solution (0.5 mg/mL) was added to each well and incubated at 37 °C for 4 h. The supernatant was then removed, and 200 µl of DMSO was added to dissolve the formazan crystals. Optical density was quantified at a wavelength of 570 nm using Elisa Reader (BioTek Instruments, Inc. USA) [21]. Dose-response curve and IC50 value were determined using GraphPad Prism software. Each experiment was performed at least in triplicate three times in an independent manner, and the mean of these results was presented as the result [22].

2.4. Treatment of MDA-MB-231 cell line with Ag-NPs

Dynamic light scattering (DLS) analysis revealed the hydrodynamic diameter of PVP-coated Ag-NPs to be between 50 and 80 nm [20]. Based on the results of the MTT assay, an appropriate concentration of Ag-NPs was selected. Treatment of MDA-MB-231 cells was performed at a concentration close to the IC50 value (4 µg/mL) to prevent loss of cell viability due to high-dose toxicity. The untreated MDA-MB-231 cell line served as the control group [23].

2.5. Apoptosis detection by flow cytometry using annexin V/PI

To evaluate cell apoptosis, MDA-MB-231 cells were collected from untreated cells, and treated with 4 µg/mL Ag-NPs. Flow cytometry analysis was conducted after 48 h using an annexin V/PI double staining kit. In brief, after the treatment of cells with Ag-NPs, 10^4 cells/well were harvested and washed with PBS. These cells were then re-suspended in binding buffer and incubated for 20 min in darkness at 4 °C. In the following, the cells were re-suspended in 100 µl of binding buffer containing 5 µl of FITC-conjugated annexin V and incubated for 15 min at room temperature (RT). Then, the cells were washed and re-suspended in 100 µL of binding buffer containing 5 µL of PI and incubated in darkness at RT for 15 min. Flow cytometry analysis using FACSCalibur (BD Bioscience, USA) detected the fluorescence, determining the percentage of apoptotic cells. The acquired data were processed using FlowJo software ver. X.0.7 [24,25].

2.6. The effect of the Ag-NPs on cell cycle

Cell cycle analysis was performed by DNA staining with propidium iodide (PI), followed by flow cytometry analysis. MDA-MB-231 cells were seeded and treated as described above. After 48 h, the cells were harvested and fixed in 70% ethanol for 1 h at 4 °C, followed by staining with propidium iodide (PI) containing RNase solution for 30 min at 4 °C. Flow cytometry was conducted using FACS Calibur. Data were analyzed using Flowjo software.

2.7. Real-time PCR (qPCR) for determination of Bax and Bcl-2 gene expression

To assess gene expression of Bax and Bcl-2, MDA-MB-231 cells were collected from the treated and untreated cells (control) ones after 48 h and washed with PBS. Total RNA was extracted from both experimental groups using the Thermo Scientific kit (K0731). RNA concentrations were quantified twice (OD A260/280 and A260/230) using nanodrop (ND-1000, Thermo Scientific, Wilmington, DE, USA). The integrity of RNA was determined by visualizing the intact RNA bands with 2% agarose gel using electrophoresis. Considering the variation in RNA concentration between experimental groups, the concentration of RNAs was standardized before cDNA synthesis. Therefore, an equal quantity (500 ng) of RNAs was reverse transcribed to the cDNA using H minus first-strand cDNA synthesis kit (Fermentas, K1632) using oligo-dT and random hexamer to enhance the efficacy of synthesis. The reactions were incubated at 65 °C for 10 min and 42 °C for 60 min, and the mixture was stopped by incubating at 70 °C for 10 min [26]. The primer

Table 1
Target gene, primer sequences, and product size.

Primer set	Sequence	Tm	Product size (bp)
Bax	F: TGCCAGCAAACCTGGTGCTCA	60	243
	R: GCACTCCCGCCACAAGATG		
Bcl-2	F: CCTGTGATGACTGAGTACC	58	128
	R: GAGACAGCCAGGAAATCA		
GAPDH	F: TTGACCTCAACTACATGGTTTACA	59	126
	R: GCTCCTGGAAGATGGTGATG		

sequences were designed by Allele ID software and then analyzed by NCBI primer blast and BLAST website. The GAPDH gene served as the internal control. The primer sequences are listed in Table 1.

qRT-PCR was applied to determine the expression level of Bax and Bcl-2 using SYBR Green PCR master mix (Takara) and the Corbett Rotor-Gene™ 6000 HRM thermocycler. qPCRs were performed in a total volume of 20 μ l containing 1 μ l of cDNA, 10 μ l master mix, 2 μ l of forward and reverse primers (10 pmol), and 6 μ l of DNase/RNase free water. The amplification profile was 95 °C for 5 min for initial denaturation, followed by 40 cycles of 94 °C for 20 s and annealing/extension at 59–61 °C (based on the primer used) for 60 s. Bax and Bcl-2 gene were normalized to GAPDH to quantify gene expression. The qPCR data were then analyzed by Rotor-Gene 6000 Software to obtain CT values. Relative miRNA expression levels were quantified according to formula $2^{-\Delta\Delta CT}$. All samples were run at least in triplicates [27,28].

2.8. Western blot analysis for determination of protein expression

To identify the impact of Ag-NPs on the protein levels of AKT, p-AKT, PTEN, P53, hTERT, cyclin D1 and p-ERK and total ERK levels, Western blot analysis was conducted. Briefly, cells from the Ag-NPs treated group and the untreated control were harvested, washed twice with cold PBS, and then lysed using RIPA buffer at 4° for 30 min. The lysate underwent centrifugation at 13000 \times g for 20 min at 4 °C, and protein concentrations in the supernatant were measured using a BCL kit (Pierce, Rockford, IL, USA). 50 μ g of each protein sample was loaded onto 12% SDS-PAGE for protein separation.

Subsequently, the proteins were transferred to a PVDF membrane and blocked with 5% skim milk (in PBS) to prevent nonspecific protein binding. Following 60 min of incubation at 25 °C, the membranes were exposed to primary antibodies (AKT, p-AKT, PTEN, P53, hTERT, cyclin D1 and p-ERK, total ERK and β -actin) (Santa Cruz) at 1:1000 dilution targeting specific proteins and kept overnight at 4 °C. After two washes, the membranes were incubated with an HRP-conjugated antibody as a secondary antibody (1:1000) (Santa Cruz) at RT for 60 min to detect the binding of primary antibodies. Finally, protein bands were visualized using enhanced chemiluminescence (ECL) (Roche, UK) and X-ray film. ImageJ 1.6 software was used to quantify band intensities, normalized to the respective β -actin protein levels as the internal control [29].

2.9. ELISA assay for determining of CyclinD1 and ERK (1/2) levels

To evaluate the intracellular levels of cyclin D1 protein and the contents of total and phosphorylated ERK1/2 in Ag-NPs treated cells, ELISA assay was conducted using PathScan® ELISA kits. Total p44/42 MAPK (Erk1/2) (Cat. # 7050C), Phospho-p44/42 MAPK (Thr202/Tyr204) (Cat. #7177), and Total cyclin D1 Sandwich ELISA Kit (Cat. #7918C) were provided by Cell Signaling Technology (Danvers, MA, USA). ELISA was performed according to the manufacturer's instructions. Briefly, MDA-MB-231 cells (8×10^5) were seeded in 100 mm petri dishes and incubated overnight. Subsequently, the cells were treated with 4 μ g/mL Ag-NPs for 48 h. The cells were then washed with cold PBS and lysed using a lysis buffer containing protease and phosphatase inhibitor cocktail (Sigma-Aldrich, USA) along with PMSF (Sigma-Aldrich, USA) according to the manufacturer's protocol. The cell lysates underwent centrifugation for 5 min at 10,000 \times g at 4 °C. To ensure equal total protein amounts in ELISA sample, the total protein concentrations in cell lysates were determined using a Pierce BCA Protein Assay Kit (Thermo Fisher Scientific, Waltham, MA, USA). Optical density was quantified using an ELISA Reader (BioTek Instruments, Inc. USA) [30].

2.10. Wound-healing assay to determine the effect of Ag-NPs on the cell migration

To elucidate the impact of Ag-NPs on cell migration of MDA-MB-231 cells, a wound-healing assay was carried out. The cells were seeded in 6 well plates (4×10^5 cells/well) and grown to reach 90% confluent monolayer. A scratch manually was made at the center of the well with a sterile micropipette tip and washed with DPBS (Dulbecco's Phosphate Buffered Saline) to remove any cellular debris. After that, the cells were treated with Ag-NPs, and cell migration was monitored at different time points (0, 6, and 24 h). In brief, the width of the wound area was measured under an inverted microscope (KRÜSS, MBL-3200) at a magnification of 10 \times . Cell-free areas were quantified by Image J software. Each condition was evaluated in triplicate and independently repeated three times.

2.11. Statistical analysis

The results obtained were analyzed using Graph Pad Prism version 6.01. One-way analysis of variance (ANOVA) followed by post hoc Tukey's tests determined any significant differences among the studied groups. Statistical significance was set at * $p < 0.05$. All experimental procedures were replicated three times.

3. Results

3.1. Effect of Ag-NPs on MDA-MB-231 cell line proliferation

MTT assay was performed to determine the optimal concentration of Ag-NPs and quantify cell viability. MDA-MB-231 cells were exposed to varied concentrations of Ag-NPs for 48 h, and then proliferation was assessed by MTT assay according to the method described by Fathi et al. [31]. Fig. 1A depicts a dose-response curve illustrating the inhibitory effects of Ag-NPs on MDA-MB-231. Based on the acquired results, the IC50 value for Ag-NPs in MDA-MB-231 cells was 3.99 ± 0.51 μ g/ml. Fig. 1B demonstrates that

concentrations of 2, 4, and 6 $\mu\text{g/ml}$ of Ag-NPs significantly reduced cell viability in MDA-MB-231 cells compared to the untreated control group ($p < 0.001$). A concentration of 4 $\mu\text{g/ml}$ of Ag-NPs was used to treat cancer cells in subsequent experiments.

3.2. Ag-NPs enhance apoptosis in MDA-MB-231 cells

To study the potential of Ag-NPs treatment in inducing or enhancing apoptosis in MDA-MB-231, annexin V/PI staining was performed using flow cytometry. Fig. 2(A) and (B) depict the contour diagram and bar graph of the annexin V/PI double staining assay of MDA-MB-231 cells. Fig. 2B displays a substantial increase in the rate of apoptosis (Annexin⁺, PI⁻) in Ag-NPs treated cells, indicating 55.48 ± 4.6 ($p < 0.001$).

3.3. Effect of Ag-NPs on cell cycle

Effects of Ag-NPs on the cell cycle in MDA-MB 231 cells was determined by flow cytometry as representatively depicted in Fig. 3A. The cell cycle analysis showed alteration in the cell cycle distributions of MDA-MB 231. 48 h after the Ag-NPs treatment (4 $\mu\text{g/ml}$), 55.38 ± 2.41 % of the MDA-MB 231 cells were in G1 phase, 15.7 ± 1.45 % were in S phase, and 26.68 ± 2.17 % were in G2 phase compared to the control group consisting of 73.52 ± 3.33 % of the cells in G1 phase, 1.4 ± 0.3 % in S phase, and 24.56 ± 3.3 % in G2 phase (Fig. 3B). The percentage of cells in the G1 and S phase was increased upon treatment with Ag-NPs. These results implied that Ag-NPs suppress cell cycle progression.

On the other hand, the apoptotic cells observed in the previous experiment (Fig. 2) were slight in this graph (Fig. 3A). This can be attributed to the DNA loss during permeation and fixation of the cells in ethanol prior to PI staining. Indeed, over 30% of total DNA is fragmented to low-molecular weight and released from the apoptotic nuclei [32].

3.4. Ag-NPs increased Bax and decreased Bcl-2 levels in MDA-MB-231 cells

Bcl-2 and Bax proteins regulate mitochondrial function and apoptosis [33]. Real-time PCR analysis was performed to identify the potential effect of Ag-NPs on the expression of pro-apoptotic (Bax) and anti-apoptotic (Bcl-2) gene. As shown in Fig. 4A, there was a significant rise in Bax levels in the cells treated with Ag-NPs (4 $\mu\text{g/ml}$) compared to the untreated control group ($p < 0.01$), while the expression level of Bcl-2 decreased notably in cells exposed to Ag-NPs ($p < 0.01$). In addition, Ag-NPs treatment markedly elevated the Bax/Bcl-2 ratio compared to that in the control group ($p < 0.001$) (Fig. 4B).

3.5. Ag-NPs induced alterations in the protein level of AKT, p-AKT, PTEN, P53, and hTERT

Several studies have shown the correlation between active p-AKT and reduced survival rates among cancer patients [14]. PTEN plays a crucial role in the proliferation and migration of breast cancer cells by negatively regulating the PI3K/AKT cascades [15]. To elucidate the signaling pathways impacting MDA-MB-231 cells, Western blot analysis assessed AKT, p-AKT, PTEN, P53, and hTERT expression levels (Fig. 5A)(Sup.1). Fig. 5B demonstrates a significant increase in PTEN level, a tumor suppressor commonly inactivated in cancers. P53, is known to regulate PTEN at transcriptional and protein levels. Fig. 5C demonstrates significant increase of P53 expression in the cells treated with Ag-NP as compared to untreated control group ($p < 0.001$). Treatment with Ag-NP led to reduced h-TERT protein levels compared to the control group ($p < 0.01$) (Fig. 5D). In addition, the ratio of p-AKT to total AKT expression was significantly reduced in MDA-MB-231 cells treated with Ag-NPs ($P < 0.05$) (Fig. 5E).

3.6. Ag-NPs decreased the expression level of cyclin D1 and phosphorylated-ERK1/2 levels in MDA-MB-231 cells

Cyclin D1 is identified as an essential protein in regulating cell cycle phases (specifically, transitioning from G1 to S) and is often

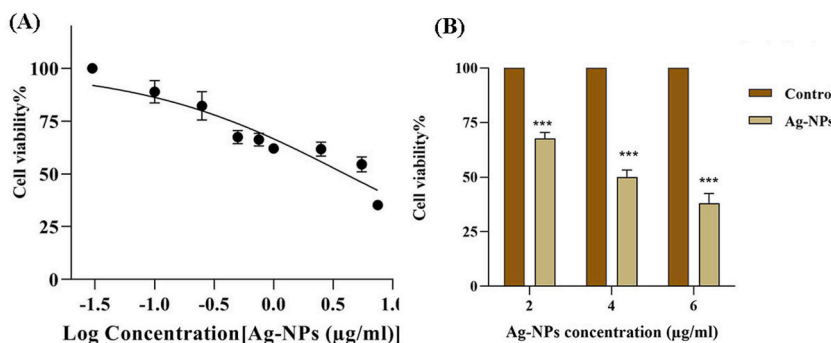


Fig. 1. (A) Dose-response curve of Ag-NPs in MDA-MB-231. A dose-response curve was constructed using GraphPad prism to calculate the IC50 value. (B) Cell viability of Ag-NPs in three different concentrations. All experiments were repeated at least three times and were reported as mean \pm SD (standard deviation). * Indicates significant comparison vs. control group. *** $p < 0.001$.

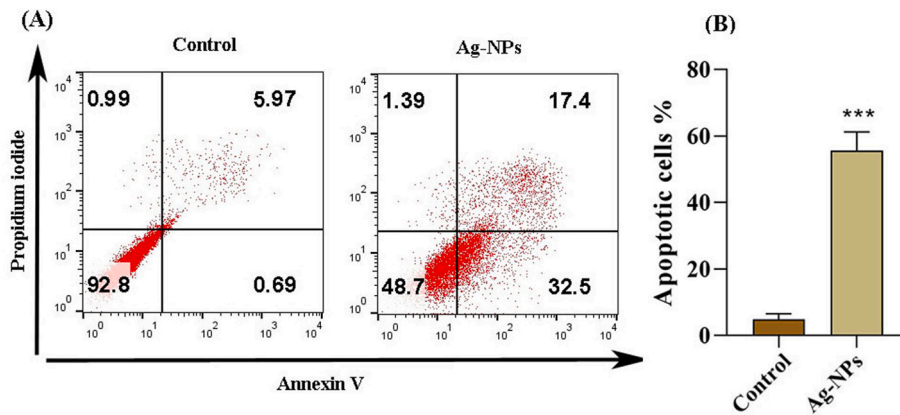


Fig. 2. Determination of apoptosis by using Annexin V/PI staining assay (A) Representative dot plot and (B) Graph bar of apoptotic MDA-MB-231 cells treated with 4 $\mu\text{g/ml}$ Ag-NPs. The assay was conducted in three independent experiments, and data were shown as mean \pm standard deviation (SD). *Indicates significant comparison vs. control group. *** $p < 0.001$.

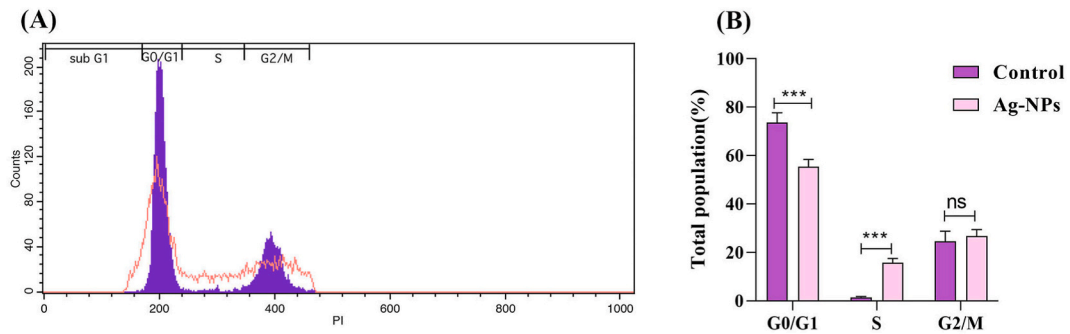


Fig. 3. The percentage of MDA-MB-231 cells at each cell cycle phase. (A) Representative histogram, and (B) bar graph of cell population in each phase of cell cycle. The cells were incubated with 4 $\mu\text{g/ml}$ Ag-NPs, and cell distribution was determined in different cell cycle phases using flow cytometry. Compared to the non-treated control group, Ag-NPs decreased the proportion of the cells in the G0/G1, and increased the proportion in the S phase. Each experiment was repeated three times. (***) $p < 0.001$.

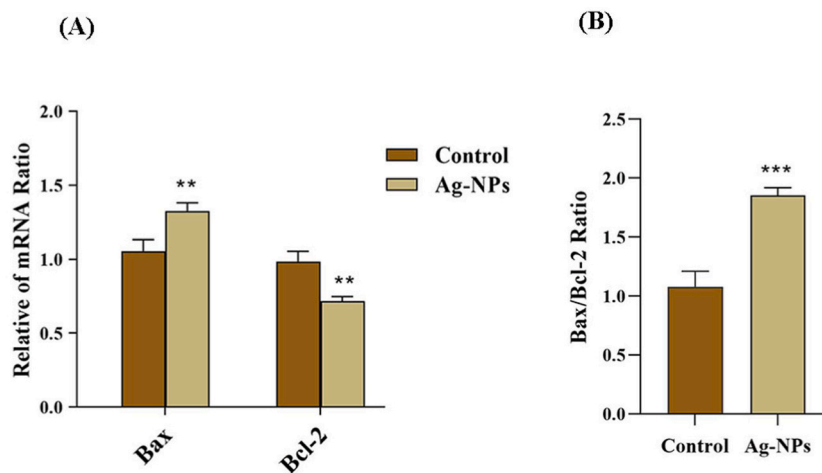


Fig. 4. The mRNA expression levels of (A) Bax and Bcl-2, (B) and the Bax/Bcl-2 ratio in MDA-MB-231 cells after treatment with 4 $\mu\text{g/ml}$ Ag-NPs were determined using real-time PCR. The mean \pm SD was calculated from three independent experiments. ** $p < 0.01$, and *** $p < 0.001$ vs. control.

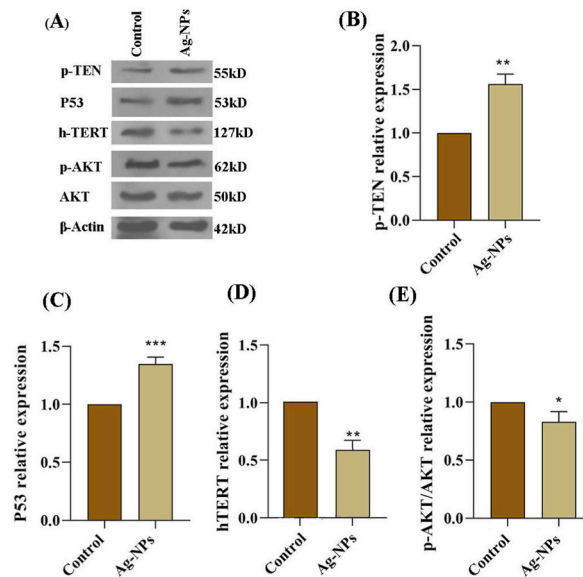


Fig. 5. Western blotting analysis of PTEN, p53, h-TERT and P-AKT expression in MDA-MB-231 cells exposed to 4 $\mu\text{g}/\text{ml}$ Ag-NPs. (A) Representative analysis, (B) PTEN (C) P53, (D) hTERT, and (E) p-AKT/AKT relative expression. All experiments were repeated three times, and data were shown as mean \pm SD. * $p < 0.05$, ** $p < 0.01$, and *** $p < 0.001$. The uncropped version of western blotting analysis was presented in Sup.1.

overexpressed in most cancer cells, such as MDA-MB-231 cells [34]. The ERK signaling pathway is crucial in cell survival and proliferation [35]. In addition, an activated form of ERK is one of the important signals associated with the resistance of MDA-MB-231 cancer cells toward various therapies such as radiotherapy. This study involved an assessment of intracellular cyclin D1 levels and phosphorylated ERK1/2 (p-ERK1/2) in the MDA-MB-231 cells using their specific ELISA kits. Fig. 6 A shows a notable reduction in the expression level of cyclin D1 in MDA-MB-231 cells exposed to Ag-NPs compared to the control group, suggesting the potential role of Ag-NPs in cell cycle arrest ($p < 0.01$). In addition, exposure to Ag-NPs (4 $\mu\text{g}/\text{ml}$) resulted in a significant reduction of p-ERK/Total ERK levels in MDA-MB-231 cells ($p < 0.01$) (Fig. 6 B). To confirm obtained results by ELISA assay, the expression level of cyclin D1 and p-ERK/total ERK levels was also assessed by western blotting analysis. As depicted in Fig. 6C (Sup.2), treatment with Ag-NPs reduced protein level of Cyclin D1 compared to the control group. In addition, the expression level of p-ERK decreased in MDA-MB-231 cells treated with Ag-NPs.

3.7. Ag-NPs inhibit the migration of MDA-MB-231 cells

The imperative characteristic of metastasis is the migration of tumor cells. To further evaluate the impact of Ag-NPs against cancer

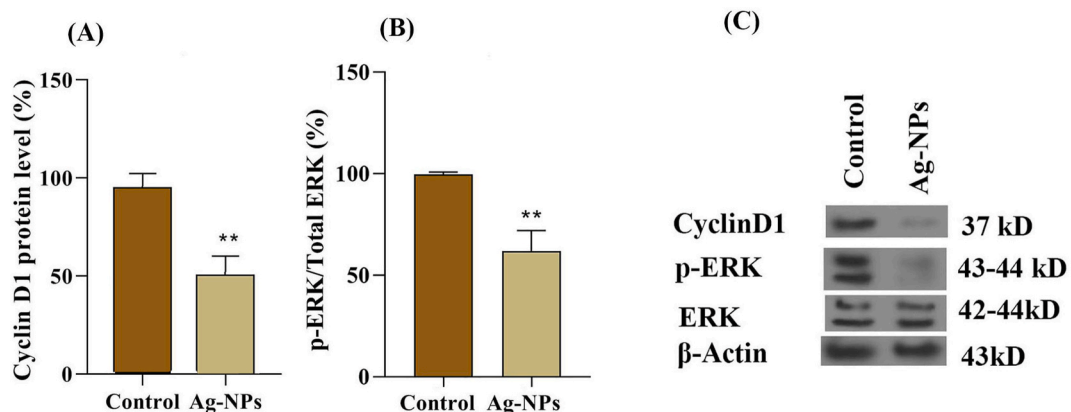


Fig. 6. ELISA (A and B) and western blotting (C) analysis of cyclin D1 protein, phosphorylated and total ERK1/2 level in MDA-MB cells exposed to 4 $\mu\text{g}/\text{ml}$ Ag-NPs for 48 h. ELISA and western blotting analysis showed reduced cyclin D1 and p-ERK protein levels in the cells treated with Ag-NPs. The experiments were repeated three times, and data were shown as mean \pm SD. ** depicts $p < 0.01$. The uncropped version of western blotting analysis was presented in Sup.2.

metastasis in MDA-MB-231 cells, we conducted cell migration analysis using the wound-healing assay. As shown in Fig. 7, Ag-NPs significantly reduced cell motility. Treatment of the MDA-MB-231 cells with Ag-NPs for 24 h inhibited cell migratory ability. The migration inhibitory effect was shown by calculating cell-free areas. Indeed, the Ag-NP-treated cells migrated less than that of the control group and weakened the migration of MDA-MB-231 cells indicated with high cell-free areas ($80.12 \pm 6.12\%$) of Ag-NP-treated cells and low cell-free areas ($22.28 \pm 3.42\%$) of the control group in T24 compared to zero time values of each group. Taken together, these findings inferred the inhibitory effects of Ag-NPs on the migration capacity of MDA-MB-231.

4. Discussion

Selecting the most suitable material within the expanding spectrum of nanomaterials available for cancer therapy is an important task. Understanding the unique potency and toxicity profiles of diverse NPs helps us to target cancer cells precisely. Several studies have reported the anticancer efficacy of Ag-NPs against breast cancer [33,36]. These Ag-NPs have been documented to trigger cell death via the induction of oxidative stress and DNA damage within mammalian cells [37,38]. TNBC represents an aggressive subtype of breast cancer, posing a substantial challenge due to the absence of specific receptors to be targeted. In addition, TNBC often exhibits resistance against different cancer therapy modalities, including chemotherapy and radiotherapy, owing to the overexpression of certain anti-apoptotic factors [4,5]. This study evaluated the cytotoxicity of Ag-NPs and the apoptosis pathways induced by Ag-NPs in TNBC cells.

In the present study, significant toxicity of Ag-NPs was observed in MDA-MB 231 cells compared to the untreated cells. Furthermore, Ag-NPs were found to induce apoptosis in MDA-MB 231 cancer cells, a recognized mechanism of cell death in cancers. These findings align with the results of other studies, indicating the reduced cell viability in cancer cells upon exposure to Ag-NPs [13]. Previous studies have reported that Ag-NPs induce apoptotic death via endoplasmic reticulum stress in HepG2 cells [39].

Our western blotting results demonstrated that Ag-NPs increased the protein expression of p53 in MDA-MB 231 cells. The p53 is known to up-regulate genes associated with apoptosis and cell cycle arrest. p53-induced apoptosis up-regulates the expression levels of pro-apoptotic (Bax) and downregulated anti-apoptotic (Bcl-2) genes. The homodimerization of Bax promotes apoptosis, and heterodimerization of Bax with Bcl-2 prevents apoptosis, increasing cell survival. Accordingly, p53-mediated apoptosis enhances Bax/Bcl2 ratio, ultimately triggering apoptosis. Indeed, p53 acts as a direct transcriptional activator of the Bax, and inactivator of Bcl-2 [40]. In the current study, Ag-NPs treatment led to the upregulation of Bax expression and downregulation of Bcl-2 expression in MDA-MB-231 cells, suggesting that the upregulation of p53 led to the activation of downstream genes. Similarly, Darvish et al. demonstrated the reduction of Bcl-2 expression in TNBC cells exposed to Ag-NPs [41]. The increasing of Bax/Bcl-2 expression ratio indicates the activation of the caspase cascade, a pivotal pathway in apoptosis [42]. It has been shown that tumor suppressors such as p53 and PTEN regulate cell migration and division [43]. Mutation or deletion in p53 is observed in 60–80% of TNBC cases, while PTEN is deleted or lost in 25–30% of TNBC cases [44]. These alterations contribute to the aggressive nature of TNBC. TNBCs exhibit distinct subgroups based on their p53 expression status. p53-positive TNBC often displays a more aggressive phenotype compared to p53-negative TNBC [45]. PTEN is an important tumor suppressor, in which its inactivity is linked with larger tumor sizes, aggressive phenotype, and multiple lymph node metastases. PTEN can negatively regulate the TNBC progression. This can be attributed to the negative impact of PTEN on PI3K/AKT pathway [15]. The present study indicates elevated PTEN levels in Ag-NP-treated groups compared to the control group.

Research by Nedeljković found that the loss of PTEN coupled with an elevated level of PI3K and mTOR correlates with poor prognosis in TNBC patients [46]. Dysfunction of PTEN often leads to the constitutive activation of AKT, as PTEN serves as a principal negative regulator of AKT signaling [47]. The PI3K/AKT/mTOR axis is one of the critical signaling pathways responsible for chemoresistance, cell proliferation, and survival in TNBC [48]. With this notion, the upregulation of PTEN, inactivates the activity of AKT pathways. Western blot results showed the upregulation of PTEN and downregulation of AKT in the cells treated with Ag-NPs compared to the control group. It is well established that hTERT plays a pivotal role in the upregulating of telomerase activity in most human cancers. Our finding revealed that Ag-NPs reduced the expression level of h-TERT in MDA-MB 231 cells. Diverse mechanisms can influence the phosphorylation of hTERT, its translocation into the nucleus, and subsequent telomerase activity. The activated form of AKT (p-AKT) is an essential factor in h-TERT activation [49]. Consistent with this understanding, western blotting results depicted a significant reduction in the p-AKT/AKT ratio in MDA-MB-231 cells treated with Ag-NPs compared to the untreated control group. Several lines of evidence revealed that activated AKT stimulates the expression of survival transcription factors while impeding the pro-apoptotic factors [50].

ERK1/2 activation has been associated with cell survival and chemoresistance by promoting the activation of Bcl-2 and the degradation of pro-apoptotic proteins such as Bcl-2-modifying factor (BMF), Bcl2-interacting mediator of cell death (BIM), and P53 upregulated modulator of apoptosis (PUMA) [51,52]. In addition, numerous studies have reported that suppressing the ERK1/2 pathway using anticancer agents can enhance apoptosis and decrease metastasis in different cancer types. Hence, apart from the AKT pathway, suppression of ERK1/2 activation by Ag-NPs might contribute to inducing apoptosis and arresting the cell cycle. In this study, ELISA assay results showed that Ag-NPs inactivate ERK1/2, as evidenced by a marked reduction in p-ERK/total ERK levels in MDA-MB-231 cells. Our findings showed a significant decrease in cyclin D1 levels in MDA-MB-231 cells treated with Ag-NPs compared to the control group. Cyclin D1, a well-established oncogene and a critical mediator in cell cycle regulation, is overexpressed in MDA-MB231 cells [53].

The transition of cells through the G1 phase in the cell cycle is mainly mediated by the activity of cyclins. Cyclin D contributes to the progression of G1 to S phase. In other words, Cyclin D1 is the most substantial element among the oncogenic factors of cell cycle machinery. Down-regulation of cyclin D1 has important effects on the cell cycle due to its impact in controlling G1/S progression [54].

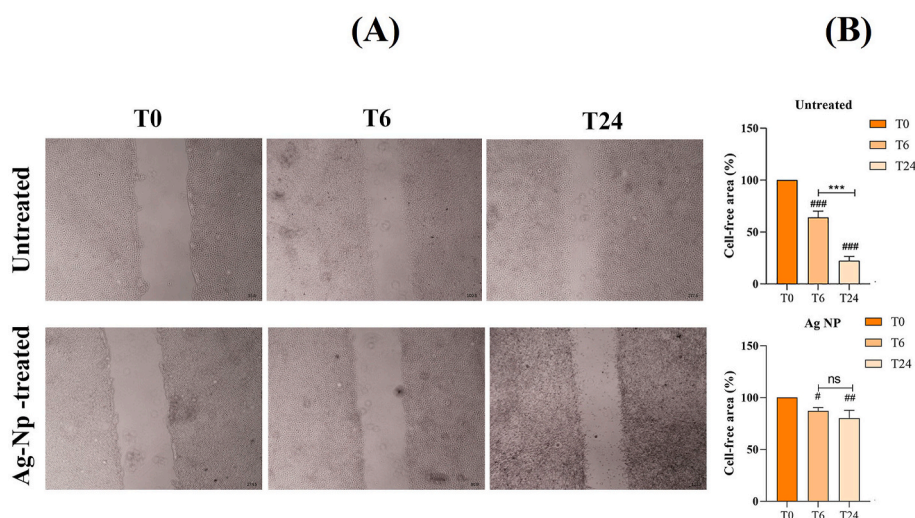


Fig. 7. Ag-NPs inhibited cell migration in MDA-MB-231 cells. The wound healing assay displayed that Ag-NPs could inhibit the migration of MDA-MB-231. (A) Representative microscopic presentation of scratched and healing of wounded areas on monolayers of cancer cells at different time points (0, 6, and 24 h) with 4 µg/ml Ag-NPs treatment. (B) Bar graph analysis of wound closure. The width of the wounds was measured to determine wound closure. The results are expressed as fold changes relative to the wound width compared to the control group. Treated cells showed lower migration capacity compared to the control cells (# $p < 0.05$, ## $p < 0.01$, and ### $p < 0.001$) (** $p < 0.001$).

Our findings is consistent with this, and reduced level of cyclin D1 is correlated with suppression of cell cycle progression.

Considering the contributory role of cell migration in cancer metastasis [55], a wound-healing assay was conducted to elucidate the migration of cancer cells upon treatment with Ag-NPs. We detected lower migration and slower healing rates of wounds in treated cells, indicating that Ag-NPs could impede the migration of MDA-MB-231 cells. These results suggest that Ag-NPs can be a promising therapeutic agent for breast cancer cell lines.

Our findings showed that Ag-NPs influenced the proliferation and apoptosis in MDA-MB 231 cells through a series of events. Although, our results provide good insights into the potential anticancer activity of Ag-NPs in MDA-MB-231, the generalizability of these findings needs to be confirmed in other cell lines particularly breast cancer cell lines. This study examined the anticancer effects of Ag-NPs as a potential therapeutic nanomedicine for the treatment of human breast cancer. The most important limitation of the employment of nanoparticles is NP-induced toxicity and related unknown immunological responses in the body. Further investigations involving experimental animal models are necessary to evaluate the effects of Ag-NPs in an *in vivo* system. Further investigations are warranted to unveil the interactions between proteins in this mechanism.

5. Conclusion

The present study reveals that Ag-NPs inhibit MDA-MB231 cells by reducing cell survival and inducing apoptosis. This effect coincides with an increase in the expression levels of the P53, PTEN, and Bax and a simultaneous decrease in the expression levels of Bcl-2, as well as *p*-AKT, hTERT, *p*-ERK1/2, and cyclin D1. The current study suggested the downregulation of cyclin D1 expression upon treatment with Ag-NPs can arrest the cell cycle and impede their progression to the subsequent phases. Ag-NPs also hampered the migration of MDA-MB-231 cells.

These alterations potentially contribute to the anticancer action of Ag-NPs through modulation of Akt/ERK/Cyclin D1 axis. Consequently, these observations suggest that Ag-NPs serve as a therapeutic anticancer agent, either as a single agent or adjuvant and might be used for the prevention and treatment of TNBC.

Funding

This project was financially supported by a research grant from the Tabriz University of Medical Sciences, Tabriz, Iran (Pazhoohan ID: 68878).

Availability of data

The data sets used and/or analyzed during the current study are available from the corresponding author on reasonable request.

Ethical approval

Ethical consent was approved by an ethics committee at Tabriz University of Medical Sciences, Tabriz, Iran (Ethic Code No: IR.TBZMED.VCR.REC.1400.422).

CRediT authorship contribution statement

Soheila Montazersaheb: Writing – review & editing, Supervision, Resources, Project administration, Investigation, Conceptualization. **Raheleh Farahzadi:** Writing – review & editing, Resources, Methodology, Investigation. **Ezzatollah Fathi:** Writing – review & editing, Resources, Methodology, Investigation. **Mahsan Alizadeh:** Investigation. **Shahabaddin Abdolalizadeh Amir:** Investigation. **Alireza Khodaei Ardakan:** Investigation. **Sevda Jafari:** Validation, Investigation, Formal analysis, Data curation.

Declaration of competing interest

The authors declare that they have no known competing financial interests or personal relationships that could have appeared to influence the work reported in this paper.

Appendix A. Supplementary data

Supplementary data to this article can be found online at <https://doi.org/10.1016/j.heliyon.2024.e26959>.

References

- [1] N. Mohseni, et al., Inhibitory effect of gold nanoparticles conjugated with interferon gamma and methionine on breast cancer cell line, *Asian Pac. J. Trop. Biomed.* 6 (2) (2016) 173–178.
- [2] S.H. Hassanpour, M. Deghani, Review of cancer from perspective of molecular, *Journal of cancer research and practice* 4 (4) (2017) 127–129.
- [3] S.-L. Qiao, et al., General approach of stimuli-induced aggregation for monitoring tumor therapy, *ACS Nano* 11 (7) (2017) 7301–7311.
- [4] F. Derakhshan, J.S. Reis-Filho, Pathogenesis of triple-negative breast cancer, *Annual review of pathology* 17 (2022) 181.
- [5] F. Hossain, et al., Precision medicine and triple-negative breast cancer: current landscape and future directions, *Cancers* 13 (15) (2021) 3739.
- [6] P.R. Walker, M. Sikorska, New aspects of the mechanism of DNA fragmentation in apoptosis, *Biochem. Cell. Biol.* 75 (4) (1997) 287–299.
- [7] N. Korkmaz, et al., Biogenic silver nanoparticles synthesized via *Mimusops elengi* fruit extract, a study on antibiofilm, antibacterial, and anticancer activities, *J. Drug Deliv. Sci. Technol.* 59 (2020) 101864.
- [8] L. Zhang, et al., Nanoparticles in medicine: therapeutic applications and developments, *Clin. Pharmacol. Ther.* 83 (5) (2008) 761–769.
- [9] L. Xu, et al., Silver nanoparticles: synthesis, medical applications and biosafety, *Theranostics* 10 (20) (2020) 8996.
- [10] A. Ehsani, et al., Nanomaterials and stem cell differentiation potential: an overview of biological aspects and biomedical efficacy, *Curr. Med. Chem.* 29 (10) (2022) 1804–1823.
- [11] V. De Matteis, et al., Silver nanoparticles: synthetic routes, in vitro toxicity and theranostic applications for cancer disease, *Nanomaterials* 8 (5) (2018) 319.
- [12] C. Ong, et al., Silver nanoparticles in cancer: therapeutic efficacy and toxicity, *Curr. Med. Chem.* 20 (6) (2013) 772–781.
- [13] M.H. Sangour, et al., Effect of Ag nanoparticles on viability of MCF-7 and Vero cell lines and gene expression of apoptotic genes, *Egyptian Journal of Medical Human Genetics* 22 (2021) 1–11.
- [14] R.L. Costa, H.S. Han, W.J. Gradishar, Targeting the PI3K/AKT/mTOR pathway in triple-negative breast cancer: a review, *Breast Cancer Res. Treat.* 169 (2018) 397–406.
- [15] C. Chai, et al., Regulation of the tumor suppressor PTEN in triple-negative breast cancer, *Cancer Lett.* 527 (2022) 41–48.
- [16] R. Hannen, J.W. Bartsch, Essential roles of telomerase reverse transcriptase hTERT in cancer stemness and metastasis, *FEBS Lett.* 592 (12) (2018) 2023–2031.
- [17] R. Roskoski Jr., ERK1/2 MAP kinases: structure, function, and regulation, *Pharmacol. Res.* 66 (2) (2012) 105–143.
- [18] J. Oba, et al., Expression of c-Kit, p-ERK and cyclin D1 in malignant melanoma: an immunohistochemical study and analysis of prognostic value, *J. Dermatol. Sci.* 62 (2) (2011) 116–123.
- [19] J. Pawlonka, B. Rak, U. Ambroziak, The regulation of cyclin D promoters—review, *Cancer Treatment and Research Communications* 27 (2021) 100338.
- [20] K. Adibkia, et al., Silver nanoparticles induce the cardiomyogenic differentiation of bone marrow derived mesenchymal stem cells via telomere length extension, *Beilstein J. Nanotechnol.* 12 (1) (2021) 786–797.
- [21] O. Molavi, et al., Chemical compositions and anti-proliferative activity of the aerial parts and rhizomes of squirting cucumber, *Cucurbitaceae*, *Jundishapur J. Nat. Pharm. Prod.* 15 (1) (2020).
- [22] A. Farjami, et al., Evaluation of the physicochemical and biological stability of cetuximab under various stress condition, *J. Pharm. Pharmaceut. Sci.* 22 (2019) 171–190.
- [23] S. Jafari, et al., Silibinin induces immunogenic cell death in cancer cells and enhances the induced immunogenicity by chemotherapy, *Bioimpacts: BI* 13 (1) (2023) 51.
- [24] S. Montazersaheb, et al., Prolonged incubation with Metformin decreased angiogenic potential in human bone marrow mesenchymal stem cells, *Biomed. Pharmacother.* 108 (2018) 1328–1337.
- [25] B. Valipour, et al., Cord blood stem cell derived CD16+ NK cells eradicated acute lymphoblastic leukemia cells using with anti-CD47 antibody, *Life Sci.* 242 (2020) 117223.
- [26] S. Montazersaheb, et al., Targeting TdT gene expression in Molt-4 cells by PNA-octaarginine conjugates, *Int. J. Biol. Macromol.* 164 (2020) 4583–4590.
- [27] S. Jafari, et al., Synergistic effect of chrysin and radiotherapy against triple-negative breast cancer (TNBC) cell lines, *Clin. Transl. Oncol.* (2023) 1–10.
- [28] S. Montazersaheb, et al., The synergistic effects of betanin and radiotherapy in a prostate cancer cell line: an in vitro study, *Mol. Biol. Rep.* (2023) 1–8.
- [29] M. Rahimi, et al., Renoprotective effects of prazosin on ischemia-reperfusion injury in rats, *Hum. Exp. Toxicol.* 40 (8) (2021) 1263–1273.
- [30] E. Fathi, et al., Mesenchymal stem cells promote caspase-3 expression of SH-SY5Y neuroblastoma cells via reducing telomerase activity and telomere length, *Iranian journal of basic medical sciences* 24 (11) (2021) 1583.
- [31] E. Fathi, et al., Cardiac differentiation of bone-marrow-resident c-kit+ stem cells by L-carnitine increases through secretion of VEGF, IL6, IGF-1, and TGF- β as clinical agents in cardiac regeneration, *J. Biosci.* 45 (1) (2020) 1–11.
- [32] G. Banfalvi, Methods to detect apoptotic cell death, *Apoptosis* 22 (2) (2017) 306–323.

- [33] Y. Tsumimoto, Role of Bcl-2 family proteins in apoptosis: apoptosomes or mitochondria? *Gene Cell.* 3 (11) (1998) 697–707.
- [34] C. Choi, et al., Cyclin D1 is associated with radiosensitivity of triple-negative breast cancer cells to proton beam irradiation, *Int. J. Mol. Sci.* 20 (19) (2019) 4943.
- [35] Y.J. Guo, et al., ERK/MAPK signalling pathway and tumorigenesis, *Exp. Ther. Med.* 19 (3) (2020) 1997–2007.
- [36] M. Jeyaraj, et al., Biogenic silver nanoparticles for cancer treatment: an experimental report, *Colloids Surf. B Biointerfaces* 106 (2013) 86–92.
- [37] Y.-H. Hsin, et al., The apoptotic effect of nanosilver is mediated by a ROS-and JNK-dependent mechanism involving the mitochondrial pathway in NIH3T3 cells, *Toxicol. Lett.* 179 (3) (2008) 130–139.
- [38] H.K. Lim, P. Asharani, M.P. Hande, Enhanced genotoxicity of silver nanoparticles in DNA repair deficient mammalian cells, *Front. Genet.* 3 (2012) 104.
- [39] Y. Cao, et al., A review of endoplasmic reticulum (ER) stress and nanoparticle (NP) exposure, *Life Sci.* 186 (2017) 33–42.
- [40] B.J. Aubrey, et al., How does p53 induce apoptosis and how does this relate to p53-mediated tumour suppression? *Cell Death Differ.* 25 (1) (2018) 104–113.
- [41] S. Darvish, et al., Silver nanoparticles: biosynthesis and cytotoxic performance against breast cancer MCF-7 and MDA-MB-231 cell lines, *Nanomedicine Research Journal* 7 (1) (2022) 83–92.
- [42] J. Baharara, et al., Silver nanoparticles biosynthesized using *Achillea biebersteinii* flower extract: apoptosis induction in MCF-7 cells via caspase activation and regulation of Bax and Bcl-2 gene expression, *Molecules* 20 (2) (2015) 2693–2706.
- [43] Z. Jiang, et al., RB1 and p53 at the crossroad of EMT and triple-negative breast cancer, *Cell Cycle* 10 (10) (2011) 1563–1570.
- [44] J.C. Liu, et al., Combined deletion of P ten and p53 in mammary epithelium accelerates triple-negative breast cancer with dependency on e EF 2 K, *EMBO Mol. Med.* 6 (12) (2014) 1542–1560.
- [45] D. Coradini, et al., p53 status identifies triple-negative breast cancer patients who do not respond to adjuvant chemotherapy, *Breast* 24 (3) (2015) 294–297.
- [46] M. Prvanović, et al., Role of PTEN, PI3K, and mTOR in triple-negative breast cancer, *Life* 11 (11) (2021) 1247.
- [47] Brigham, et al., Comprehensive molecular portraits of human breast tumours, *Nature* 490 (7418) (2012) 61–70.
- [48] D. Massihnia, et al., Triple negative breast cancer: shedding light onto the role of pi3k/akt/mTOR pathway, *Oncotarget* 7 (37) (2016) 60712.
- [49] D.-O. Moon, et al., Gefitinib induces apoptosis and decreases telomerase activity in MDA-MB-231 human breast cancer cells, *Arch Pharm. Res. (Seoul)* 32 (2009) 1351–1360.
- [50] B.D. Manning, A. Toker, AKT/PKB signaling: navigating the network, *Cell* 169 (3) (2017) 381–405.
- [51] S.J. Cook, et al., Control of cell death and mitochondrial fission by ERK 1/2 MAP kinase signalling, *FEBS J.* 284 (24) (2017) 4177–4195.
- [52] N.J. Darling, K. Balmanno, S.J. Cook, ERK1/2 signalling protects against apoptosis following endoplasmic reticulum stress but cannot provide long-term protection against BAX/BAK-independent cell death, *PLoS One* 12 (9) (2017) e0184907.
- [53] D.M. Barnes, C.E. Gillett, Cyclin D1 in breast cancer, *Breast Cancer Res. Treat.* 52 (1998) 1–15.
- [54] L. Ding, et al., The roles of cyclin-dependent kinases in cell-cycle progression and therapeutic strategies in human breast cancer, *Int. J. Mol. Sci.* 21 (6) (2020) 1960.
- [55] C.D. Paul, P. Mistriotis, K. Konstantopoulos, Cancer cell motility: lessons from migration in confined spaces, *Nat. Rev. Cancer* 17 (2) (2017) 131–140.